Matrix-Isolation FT−IR Studies and Theoretical Calculations of Hydrogen-Bonded Complexes of Molecules Modeling Adenine Tautomers. 1. H-Bonding of Benzimidazoles with H_2O in Ar Matrices

Kristien Schoone,[†,‡] Johan Smets,[†,§] Linda Houben,[†] Marlies K. Van Bael,[†] Ludwik Adamowicz,[*,§] and Guido Maes[†,‡,||]

Department of Chemistry, University of Leuven, Celestijnenlaan 200F, B-3001 Heverlee, Belgium, and Department of Chemistry, University of Arizona, Tucson, Arizona 85721

Received: December 2, 1997; In Final Form: April 7, 1998

This work opens a series of studies on the water complexes of adenines. We use a similar approach as used in our earlier studies of cytosine−water complexes (i.e., first we investigate the IR spectral manifestations of hydrogen−bonding at selected interaction sites of the stable amino N_9H tautomeric form of adenine by studying simpler model molecules which have only a single or a very few selected hydrogen-bond interaction sites typical for adenine). The present study concerns the first two of such model molecules, benzimidazole and 1-CH_3−benzimidazole. IR vibrational spectra of matrix-isolated benzimidazole, 1-CH_3−benzimidazole, and their complexes with water are analyzed and assigned by comparing the experimental spectra with the IR frequencies and intensities computed with the use of ab initio and density functional theory (DFT) methods. When the DFT/B3LYP/6-31++G** monomer frequencies are scaled with three different scaling factors, the mean differences between the experimental and calculated frequencies are only 10 and 8 cm^{-1} for benzimidazole and 1-CH_3−benzimidazole, respectively. The calculated, MP2/6-31++G**//RHF/6-31++G** (MP2 denotes the second-order Møller−Plesset Perturbation Theory, RHF denotes the restricted Hartree-Fock method, and notation MP2//RHF denotes that the molecular geometries were optimized at the RHF level and then used to calculate total energies using the MP2 method), H-bond interaction energies, with the basis set superposition error accounted for, are −22.6, −21.2, and −22.0 kJ/mol for the benzimidazole N_1−H···OH_2 and N_3···H−OH complexes and the 1-CH_3−benzimidazole N_3···H−OH complex, respectively. The DFT/B3LYP/6-31++G** method yields similar H-bond interaction energies. The frequency shifts of the vibrational modes directly involved in the H-bond interactions are better predicted by the DFT method than by the RHF method. For other vibrational modes not directly involved in the H-bonds, the two methods provide a similar level of accuracy in predicting the shifts of the fundamental modes caused by H-bonding interactions. In this work we also establish correlations between experimental and theoretical characteristics of the N−H···OH_2 H-bonding in water complexes of benzimidazole and 1-CH_3−benzimidazole, and these correlations will be used in future elucidation of FT−IR spectra of water complexes of adenine.

1. Introduction

Hydrogen bonding in pairs of nucleic acid bases (NAB) forming DNA and RNA biopolymers is one of the most important examples of intermolecular interactions with significant biological implications. The hydrogen-bond interactions facilitate fidelity of replication of genetic information and are involved in the transcription processes in molecular biology.[1,2] Prototropy of NABs leads to occurrence of the NAB molecules in different tautomeric forms. Different tautomers usually have different H-bonding interaction centers and may exhibit significant differences in their H-bond characteristics. This link between the tautomerism of NABs and their H-bonding properties is of primary importance, since "abnormal pairing" through H-bond interactions of minor tautomeric forms may lead to mutations.[3,4] This possibility has motivated numerous experimental and theoretical studies on tautomerism, H-bonding, and association of NABs.[5−18]

In the former series of reports,[5−11] we have demonstrated that matrix-isolation FT−IR spectrometry coupled with ab initio calculations is an effective approach to qualitatively and quantitatively describe the tautomeric and H-bonding behavior of cytosine and isocytosine. In our work we first applied the approach to a series of model molecules with increasing tautomeric and H-bonding complexity which model the various H-bond interaction centers of the cytosine tautomers. Then we developed a series of correlations between experimental observed IR frequency shifts and such theoretically determined quantities as H-bond interaction energies, proton affinities, etc. These correlations have been extremely useful in interpretation and elucidation of the FT−IR spectra of water complexes of cytosine isolated in Ar matrixes.[5−11,17,18] Similar correlations are developed in the present work for N−H···OH_2 type systems modeling H-bonding interaction sites of adenine and adenine derivatives.

The tautomerism in adenine is either of the amino−imino or the $N_iH \rightleftharpoons N_jH$ (i, j = 1, 3, 7, or 9) type. As a result, adenine

* Corresponding author.
† University of Leuven.
‡ Research Assistant of the Flemish Fund for Scientific Research (FWO).
§ University of Arizona.
|| Senior Research Associate of the Flemish Fund for Scientific Research (FWO).

S1089-5639(98)00373-9 CCC: $15.00 © 1998 American Chemical Society
Published on Web 06/05/1998

TABLE 1: Internal Coordinates[a] Used in the Normal Mode Analysis for Benzimidazole (A), Benzimidazole···Water:N_3···HOH Complex (B), and N_1H···OH_2 Complex (C)

A	
$S_1 = r_{1,2}$	$\nu(N_1C_2)$
$S_2 = r_{2,3}$	$\nu(C_2C_3)$
$S_3 = r_{3,9}$	$\nu(N_3C_9)$
$S_4 = r_{9,4}$	$\nu(C_4C_9)$
$S_5 = r_{4,5}$	$\nu(C_4C_5)$
$S_6 = r_{5,6}$	$\nu(C_5C_6)$
$S_7 = r_{6,7}$	$\nu(C_6C_7)$
$S_8 = r_{7,8}$	$\nu(C_7C_8)$
$S_9 = r_{8,9}$	$\nu(C_8C_9)$
$S_{10} = r_{8,1}$	$\nu(C_8N_1)$
$S_{11} = r_{11,10}$	$\nu(N_1H)$
$S_{12} = r_{2,11}$	$\nu(C_2H)$
$S_{13} = r_{4,12}$	$\nu(C_4H)$
$S_{14} = r_{5,13}$	$\nu(C_5H)$
$S_{15} = r_{6,14}$	$\nu(C_6H)$
$S_{16} = r_{7,15}$	$\nu(C_7H)$
$S_{17} = (2.5^{-1/2})(\delta_{1,2,8} + a(\delta_{1,2,3} + \delta 1,8,9) + b(\delta_{2,3,9} + \delta_{3,8,9}))$ (°°)	δ_{r1}
$S_{18} = (1/3)(((a - b)(\delta_{1,8,9} + \delta_{1,2,3})) + ((1 - a)(\delta_{2,3,9} - \delta_{3,8,9})))$ (°°)	δ_{r2}
$S_{19} = (6^{-1/2})(\delta_{4,5,6} - \delta_{5,6,7} + \delta_{6,7,8} - \delta_{4,5,9} + \delta_{4,8,9} - \delta_{7,8,9})$	δ_{R1}
$S_{20} = (8^{-1/2})(-\delta_{4,5,6} - \delta_{5,6,7} + 2\delta_{6,7,8} + 2\delta_{4,5,9} - \delta_{4,8,9} - \delta_{7,8,9})$	δ_{R2}
$S_{21} = (1/4)(\delta_{5,6,7} - \delta_{4,5,6} + \delta_{4,8,9} - \delta_{7,8,9})$	δ_{R3}
$S_{22} = (2^{-1/2})(\delta_{1,8,10} - \delta_{1,2,10})$	$\delta(N_1H)$
$S_{23} = (2^{-1/2})(\delta_{2,3,11} - \delta_{1,2,11})$	$\delta(C_2H)$
$S_{24} = (2^{-1/2})(\delta_{5,4,12} - \delta_{9,4,12})$	$\delta(C_4H)$
$S_{25} = (2^{-1/2})(\delta_{6,5,13} - \delta_{4,5,13})$	$\delta(C_5H)$
$S_{26} = (2^{-1/2})(\delta_{7,6,14} - \delta_{5,6,14})$	$\delta(C_6H)$
$S_{27} = (2^{-1/2})(\delta_{8,7,15} - \delta_{6,7,15})$	$\delta(C_7H)$
$S_{28} = (1/3)((a - b)(\tau_{1,3,8,9} - \tau_{1,2,3,9}) + (1 - a)(\tau_{1,2,3,8} - \tau_{1,2,8,9}))^b$	τ_{r1}
$S_{29}(2.5^{-1/2})(\tau_{1,2,3,9} + b(\tau_{1,2,8,9} + \tau_{1,2,3,8}) + a(\tau_{1,3,8,9} + \tau_{1,2,3,9}))$	τ_{r2}
$S_{30} = (6^{-1/2})(\tau_{4,5,6,7} - \tau_{4,5,6,8} + \tau_{4,7,8,9} + \tau_{6,7,8,9} - \tau_{5,6,7,8})$	τ_{R1}
$S_{31} = (1/2)(\tau_{8,9,4,5} - \tau_{6,7,8,9} - \tau_{5,6,7,8} - \tau_{4,5,6,9})$	τ_{R2}
$S_{32} = (8^{-1/2})(2\tau_{4,5,6,7} - \tau_{5,6,7,8} - \tau_{4,5,6,9} + 2\tau_{4,7,8,9} - \tau_{4,5,8,9} - \tau_{6,7,8,9})$	τ_{R3}
$S_{33} = (2^{-1/2})(\tau_{1,8,9,4} - \tau_{3,9,8,7})$	τ_{rR}
$S_{34} = \gamma_{10,1,2,8}$	$\gamma(N_1H)$
$S_{35} = \gamma_{11,2,1,3}$	$\gamma(C_2H)$
$S_{36} = \gamma_{12,4,5,9}$	$\gamma(C_4H)$
$S_{37} = \gamma_{13,5,4,6}$	$\gamma(C_5H)$
$S_{38} = \gamma_{14,5,6,7}$	$\gamma(C_6H)$
$S_{39} = \gamma_{15,6,7,8}$	$\gamma(C_7H)$
B	
$S_{40} = (2^{-1/2})(r_{16,17} - r_{18,17})$	ν^f_{OH}
$S_{41} = (2^{-1/2})(r_{16,17} + r_{18,17})$	ν^f_{OH}
$S_{42} = r_{3,16}$	$\nu_{N\cdots OH}$
$S_{43} = \delta_{16,17,18}$	δ_{HOH}
$S_{44} = (2^{-1/2})(\delta_{16,3,2} - \delta_{16,3,9})$	$\delta_{N\cdots HO}$
$S_{45} = (2^{-1/2})(\delta_{17,3,2} - \delta_{17,3,9})$	in plane (ip) "butterfly"[c]
$S_{46} = \gamma_{17,3,2,9}$	out of plane (oop) "butterfly"[c]
$S_{47} = \gamma_{16,3,2,9}$	N···HO out of plane (oop) wag
$S_{48} = (2^{-1/2})(\tau_{18,17,3,9} + \tau_{18,17,3,2})$	HO torsion about N···OH
C	
$S_{40} = (2^{-1/2})(r_{17,16} + r_{18,16})$	ν^s_{OH}
$S_{41} = (2^{-1/2})(r_{17,16} - r_{18,16})$	ν^a_{OH}
$S_{42} = r_{1,16}$	$\nu_{N\cdots H}$
$S_{43} = \delta_{18,17,16}$	δ_{HOH}
$S_{44} = \delta_{16,1,8}$	out-of-plane (oop) "butterfly"[c]
$S_{45} = \delta_{17,1,8}$	H_2O out-of-plane (oop) translation
$S_{46} = \delta_{18,1,16}$	H_2O in-plane (ip) wag
$S_{47} = \gamma_{16,1,2,8}$	in-plane (ip) "butterfly"[c]
$S_{48} = (2^{-1/2})(\tau_{17,16,1,8} + \tau_{18,16,1,8})$	H_2O twist

[a] $r_{i,j}$ indicates stretch of $i-j$ bond, $\delta_{i,j,k}$ bend of the angle between the bonds $i-j$ and $j-k$, $\gamma_{i,j,k,l}$ bend of the bond $i-k$ out of the plane defined by the bonds $j-k$ and $i-l$, and $\tau_{i,j,k,l}$ torsion of the plane defined by the bonds $i-j$ and $j-k$ with respect to the plane defined by the bonds $j-k$ and $k-l$. [b] $a = -0.809$, $b = 0.309$. [c] Description of the coordinate according to Person et al. (ref 33).

can occur, at least in principle, in eight different tautomeric forms.[19] Recent vibrational studies in matrixes have indicated that the amino−N_9H tautomer is by far the most stable form in the isolated state.[20] This result is fully consistent with high-level ab initio predictions.[21] In the amino−N_9H tautomeric form, adenine has multiple proton−acceptor (H_2N, N_1, N_3, or N_7) and proton−donor (NH_2 or N_9H) H-bonding interaction sites. As a result, a large number of H-bonded complex species may arise from the interaction of adenine with a water molecule and they could be identified in a low-temperature, adenine/water-doped Ar matrix. For a correct interpretation of these multiple spectra, reliable information about the strength and the spectral characteristics of each of the H-bonding interaction types must be available. This information can be provided by studies of simpler model molecules containing some of the H-bonding

TABLE 2: Experimental (Ar Matrix) and Calculated (DFT/6-31++G) IR Spectral Data for Benzimidazole**

experimental	I^a	calculated ν (cm^{-1})		I			experimental	I^a		calculated ν (cm^{-1})		I		
ν (cm^{-1})	(km/mol)	*b*	*c*	(km/mol)	PED[d]		ν (cm^{-1})	(km/mol)		*b*	*c*	(km/mol)	PED[d]	
3508/3502[e]	172	3562	3487	67	$\nu(N_1H)$	100	1009	9		999	1004	7	$\nu(C_5C_6)$	45
3093	3	3155	3091	1	$\nu(C_2H)$	99							$\nu(C_4C_5)$	15
3076	13	3116	3052	10	$\nu(C_4H)$	70							$\nu(C_6C_7)$	14
					$\nu(C_5H)$	22	*f*			952	961	<1	$\gamma(C_5H)$	54
3064	1	3106	3042	20	$\nu(C_6H)$	49							$\gamma(C_6H)$	34
					$\nu(C_7H)$	23							$\gamma(C_4H)$	27
					$\nu(C_4H)$	20	949/*944*	44	21	916	925	3	$\gamma(C_4H)$	38
3052	9	3095	3031	13	$\nu(C_7H)$	46							$\gamma(C_6H)$	37
					$\nu(C_5H)$	46							$\gamma(C_7H)$	30
3033	1	3086	3022	<1	$\nu(C_6H)$	44	926	7	3	916	920	1	δ_{r1}	49
					$\nu(C_5H)$	25							δ_{r2}	21
					$\nu(C_7H)$	29							$\nu(C_8C_9)$	20
1627	10	1618	1627	8	$\nu(C_7C_8)$	23	*902*/899	25	12	839	848	8	$\gamma(C_2H)$	46
					$\nu(C_4C_5)$	13							$\gamma(C_7H)$	25
					$\nu(C_4C_9)$	13							$\gamma(C_4H)$	14
1594/*1580*	3	1580	1588	4	$\nu(C_8C_9)$	19	877	29	14	862	866	3	δ_{R1}	53
					$\nu(C_5C_6)$	16	858	18	9	827	836	5	$\gamma(C_7H)$	19
					$\nu(C_4C_9)$	17							$\gamma(C_4H)$	14
					$\nu(C_6C_7)$	10							$\gamma(C_5H)$	10
1504/*1500*	35	1495	1501	35	$\nu(C_2N_3)$	53							$\gamma(C_2H)$	58
					$\delta(C_2H)$	18	776	19	9	766	770	5	δ_{R2}	10
1494/1489	3	1480	1488	3	$\delta(C_5H)$	23							$\nu(C_4C_9)$	15
					$\delta(C_6H)$	12							$\nu(C_8C_9)$	16
					$\nu(C_4C_5)$	15	776	19	9	766	770	5	δ_{R2}	10
1454/1448	35	1439	1446	24	$\delta(C_7H)$	22							$\nu(C_4C_9)$	15
					$\delta(C_4H)$	19							$\nu(C_8C_9)$	16
					$\nu(C_8C_9)$	16	766	22	10	743	751	29	τ_{RI}	19
1396/*1392*/1384	39	1384	1391	25	$\delta(N_1H)$	29							τ_{r2}	26
					$\nu(N_1C_2)$	10							$\gamma(C_6H)$	16
					$\delta(C_6H)$	19	742	194	93	728	736	55	$\gamma(C_6H)$	16
1357/1342	30	1346	1353	36	$\nu(C_8C_9)$	14							$\gamma(C_5H)$	26
1304	12	1301	1307	9	$\delta(C_5H)$	11							τ_{R1}	19
					$\nu(N_3C_9)$	14	637	6	3	628	634	3	τ_{r1}	54
					$\delta(C_2H)$	21							τ_{r2}	33
					$\nu(C_2N_3)$	18	620	1	<1	609	612	<1	δ_{R3}	29
1274/*1265*	34	1252	1259	31	$\nu(N_3C_9)$	13							δ_{r2}	31
					$\nu(N_1C_8)$	13							δ_{r1}	16
					$\delta(C_4H)$	19	578	11	5	569	575	4	τ_{R3}	40
1256/*1253*	22	1239	1246	16	$\delta(C_7H)$	17							τ_{R1}	44
1178	<1	1170	1176	1	δ_{R1}	18							τ_{r1}	22
					$\delta(C_2H)$	21	542	2	1	534	537	<1	δ_{R2}	71
					$\nu(N_3C_9)$	12	459/*449*	228	109	425	430	72	$\gamma(N_1H)$	91
1161/*1148*	2	1138	1144	2	$\delta(C_6H)$	30	420	54	26	418	422	28	τ_{R2}	85
					$\nu(C_5C_6)$	13							τ_{rR}	10
					$\delta(C_7H)$	15	411	23	11	405	408	8	δ_{R3}	53
					$\delta(C_6H)$	30	*g*			247	249	3	τ_{R3}	61
1112	3	1098	1103	2	$\nu(C_4C_5)$	15							τ_{r2}	18
					$\delta(C_5H)$	14							τ_{r1}	16
					$\delta(C_4H)$	12	*g*			216	218	9	τ_{rR}	69
					δ_{R1}	15							τ_{R2}	22
					$\nu(C_6C_7)$	16								
1080	23	1067	1073	20	$\nu(N_1C_2)$	61								
					$\delta(N_1H)$	26								

[a] Experimental intensities normalized to the theoretical value for the 1495 cm^{-1} mode (35 km/mol). [b] Uniform scaling factor 0.97. [c] Scaling factor 0.95 for ν(XH), 0.98 for γ and τ, and 0.975 for other vibrational modes. [d] Only contributions > 10 are listed. [e] Strongest component of multiplet underlined. [f] Too weak to be observed. [g] Situated below studied region (<400 cm^{-1}).

interaction sites similar to the H-bonding sites of the most abundant adenine tautomers.

The following series of model compounds carrying an increasing number of H-bond interaction sites was chosen for this purpose:

1-CH_3−benzimidazole (N) → imidazole (N−H,N) → benzimidazole (N−H,N) → purine (N−H, N_1, N_3, N_7) → 4-NH_2−pyrimidine (N_1, N_3, NH_2) → 4-NH_2−benzimidazole (N−H, N, NH_2)

Among these model compounds, purine,[22] 4-NH_2−pyrimidine,[7] and 4-NH_2−benzimidazole[23] can occur in different tautomeric forms. The interaction between water and imidazole (IM) in Ar matrices was investigated in the former study.[24]

Benzimidazole (BIM) and 1-CH_3−benzimidazole (MBIM) may serve as models for the five-member-ring part of adenine and guanine. In MBIM only one basic site, N_3, is available for H-bonding, while there are two H-bonding sites, N_1H and N_3, in BIM which can form N_1−H···OH_2 and N_3···HO−H H-bonded complexes. To our knowledge, IR spectra of BIM were only recorded in the crystalline state,[25,26] while no IR spectral data are available for MBIM.

2. Methodology

2.1. Experimental Method. The cryogenic (Leybold RDK 89113) and FT−IR (Bruker IFS-88) equipment used in this work have been described in detail previously.[27,28] To evaporate the solid compounds BIM and MBIM, the custom-made minifurnace[28] was installed into the cryostat, and the optimal sublimation temperatures for both BIM and MBIM were found to be 30 and 15 °C, respectively, at an Ar deposition rate of 5 mmol h^{-1}. Dimerization of BIM in Ar occurs only above 35 °C.[29] Base/H_2O/Ar samples were studied at base/Ar ratios similar to those applied in the study of the monomeric compounds, while the base/H_2O ratio varied between 1:1 and 1:5. As has been demonstrated before,[5−11] the latter ratio ensures an excess amount of 1:1 base. H_2O H-bonded complexes were found to be present in the Ar matrix with only weak spectral manifestations of higher stoichiometry complexes.

The studied compounds, BIM (99%) and MBIM (99%), were purchased from from SIGMA and Aldrich Europe, respectively. Deuterated BIM-d_1 was prepared by repeatedly dissolving the parent compound in CH_3OD (aquired from JANSSEN Chimica; 99.5 *d*% pure) followed by recrystallization. Bidistilled water was used for the experiments with water-doped samples, while Ar gas of the highest purity available (99.9999%) purchased from Air Liquide was used in the experiments.

2.2. Theoretical Method. In the work on imidazole water complexes,[24] we compared the predictive abilities of different theoretical methods (RHF, MP2, and DFT) and different basis sets in reproducing the experimental matrix IR results. The purpose of this investigation was to select the most effective theoretical method for the future studies on H-bonded complexes of adenines and guanines. As expected, the study showed that the frequency shifts for the vibrational modes perturbed by the H-bond formation, ν_{OH}^{b} and ν_{NH} ..., are much better predicted when diffuse functions are added to the basis set and the electron correlation is accounted for to some degree in the calculations (by MP2 or DFT methods). For the vibrational modes not directly affected by the H-bonds, the RHF and DFT methods seem to be adequate in providing reliable frequency shifts.[24] Thus, these methods with the 6-31++G** basis set were selected for the studies of water complexes of the above-mentioned series of molecules.

The choice of the 6-31++G** basis set was based on the consideration that, in order to accurately represent the electronic structure of the monomers with special emphasis on the peripheral regions of the wave functions, which are most sensitive to weak intermolecular bonding effects, it is essential to employ sets of orbitals that possess sufficient diffuseness and angular flexibility.[30] In the study of the two isomeric H-bonded complexes of IM, we have demonstrated that the 6-31++G** basis set yields theoretical predictions of considerably better accuracy than those obtained for the 6-31G** basis.[24] In particular, addition of the diffuse functions allows a considerably better description of the long-range interaction of the H-bond.

The RHF method with the 6-31++G** basis set was used in the present study for optimizations of the structures of the free and water-complexed bases. For each system this was followed by a single-point MP2/6-31++G** calculation with the frozen core electrons option. We also applied the density functional theory (DFT) method using the hybrid of Becke's nonlocal three-parameter exchange and correlated functional with the Lee−Yang−Parr correlation functional (DFT/B3LYP).[31,32] The integration grid used in the DFT method was the so-called finegrid of the GAUSSIAN package, which consists of 75 radial shells and 302 angular points for every atom.

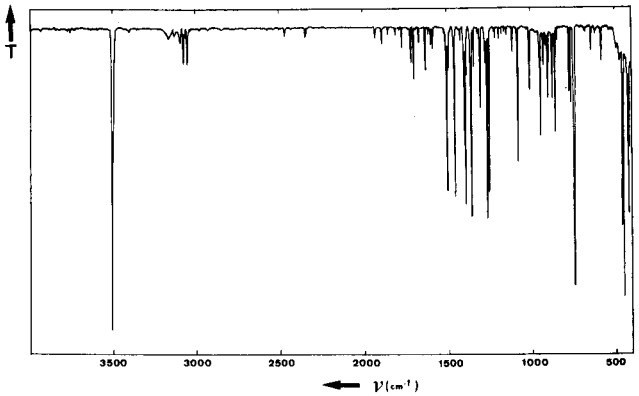

Figure 1. The FT−IR spectrum of benzimidazole in Ar at 12 K.

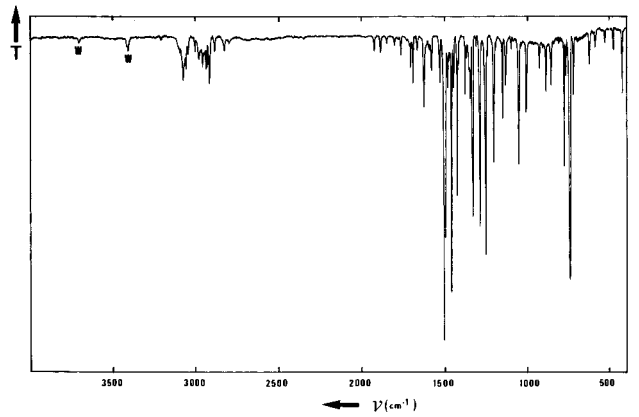

Figure 2. The FT−IR spectrum of 1-CH_3−benzimidazole in Ar at 12 K (w = water impurity).

SCHEME 1

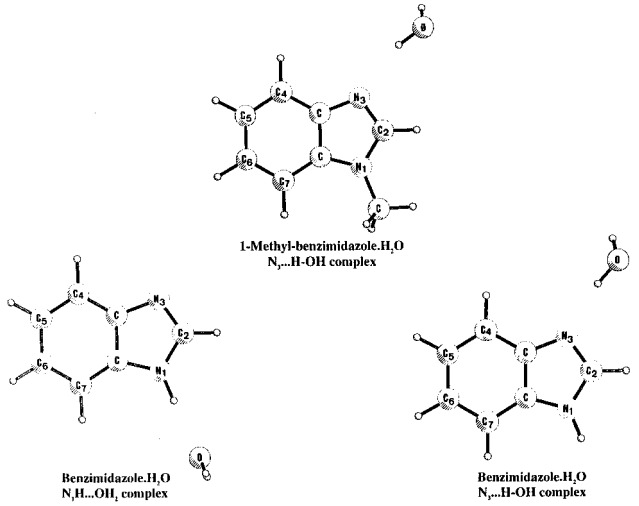

The computed total energy for each system includes the zero-point vibrational energy calculated either at the RHF level with the single scaling factor of 0.90 for all the frequencies or at the DFT level with the 0.97 scaling factor. The IR frequencies and intensities were computed at the RHF and DFT levels of theory using analytical derivative procedures implemented in the GAUSSIAN 92 and GAUSSIAN 94 programs.[33]

In the analysis of the vibrational modes, the internal coordinates were defined and used to express the molecular fixed symmetry coordinates. Then, the normal coordinates obtained

TABLE 3: Experimental (Ar Matrix) and Calculated (DFT/6-31++G) IR Spectral Data for 1-CH_3−Benzimidazole**

experimental	I^a	calculated ν (cm^{-1})		I^a			experimental	I^a	calculated ν (cm^{-1})		I^a		
ν (cm^{-1})	(km/mol)	*b*	*c*	(km/mol)	PED[d]		ν (cm^{-1})	(km/mol)	*b*	*c*	(km/mol)	PED[d]	
3072	1	3145	3080	2	$\nu(C_2H)$	99	1099/*1097*	1	1080	1085	1	δ_{R1}	31
3060	1	3116	3051	12	$\nu(C_4H)$	67	1050	22	1030	1035	21	$\rho_2(CH_3)$	30
					$\nu(C_5H)$	23						$\nu(N_1C_2)$	25
3051	1	3106	3042	21	$\nu(C_6H)$	42	1007	6	998	1003	8	$\nu(C_5C_6)$	44
					$\nu(C_7H)$	33						$\nu(C_4C_5)$	15
					$\nu(C_4H)$	20						$\nu(C_6C_7)$	13
3041	1	3096	3031	11	$\nu(C_5H)$	43	972	<1	954	963	<1	$\gamma(C_5H)$	55
					$\nu(C_7H)$	45						$\gamma(C_6H)$	32
3000	2	3086	3022	<1	$\nu(C_6H)$	47						$\gamma(C_4H)$	28
					$\nu(C_5H)$	31	926	2	914	923	3	$\gamma(C_4H)$	37
					$\nu(C_7H)$	20						$\gamma(C_6H)$	39
2955	1	3049	2986	9	$\nu^d_2(CH_3)$	72						$\gamma(C_7H)$	30
					$\nu^d_1(CH_3)$	17	886	4	868	873	3	δ_{R1}	41
2934/2928[e]	3	3008	2946	19	$\nu^d_1(CH_3)$	75						δ_{r2}	21
					$\nu^d_2(CH_3)$	25	855	6	838	847	6	$\gamma(C_2H)$	38
2913	8	2949	2888	57	$\nu^s(CH_3)$	89						$\gamma(C_7H)$	28
1624	10	1613	1621	15	$\nu(C_7C_8)$	20						$\gamma(C_4H)$	15
					$\nu(C_4C_9)$	16						$\gamma(C_5H)$	13
					$\nu(C_4C_5)$	13	840	<1	825	834	4	$\gamma(C_7H)$	15
1578	2	1576	1584	2	$\nu(C_8C_9)$	20						$\gamma(C_4H)$	12
					$\nu(C_5C_6)$	17						$\gamma(C_2H)$	66
					$\nu(C_4C_9)$	14	778	9	768	772	8	δ_{R2}	15
1503/1497[f]	86	1495	1502	86	$\nu(C_7N_3)$	43						$\nu(C_7C_8)$	15
					$\delta(C_2H)$	22						$\nu(C_4C_9)$	14
1484	4	1482	1490	12	$\delta^d_2(CH_3)$	38	*742*/740	50	730	738	73	τ_{R1}	10
					$\delta^d_1(CH_3)$	13						$\gamma(C_6H)$	22
1473	<1	1469	1475	<1	$\delta(C_6H)$	14						$\gamma(C_7H)$	14
					$\nu(C_4C_5)$	14						$\gamma(C_5H)$	28
					$\delta^d_2(CH_3)$	17	767	3	747	755	13	τ_{R1}	46
1461	32	1449	1457	33	$\delta(C_4H)$	15						τ_{r2}	31
					$\delta(C_7H)$	14	722	6	709	713	5	$\nu(N_1C)$	26
					$\nu(C_8C_9)$	12						δ_{R3}	18
1447	5	1442	1449	10	$\delta^d_1(CH_3)$	69	622	2	611	617	2	τ_{r1}	42
					$\delta^d_2(CH_3)$	23						τ_{r2}	41
1423	11	1416	1424	20	$\delta^s(CH_3)$	81						τ_{R1}	18
1378	3	1367	1374	8	$\nu(N_1C_8)$	14	583	<1	566	571	<1	τ_{R3}	37
					$\delta(C_6H)$	14						τ_{r1}	39
1346	3	1351	1358	2	$\nu(C_2N_3)$	18						τ_{R1}	34
					$\nu(N_1C_2)$	16	588	4	572	575	3	δ_{r1}	31
					$\nu(N_1C)$	12						δ_{r2}	16
1333/*1330*	29	1317	1324	34	$\nu(N_1C_2)$	12						τ_{R2}	15
					$\nu(N_1C_8)$	15						$\nu(C_7C_8)$	13
1288	28	1278	1285	35	$\nu(N_3C_9)$	29	525	1	526	528	1	δ_{R2}	52
					$\delta(C_2H)$	14	477	3	472	475	4	δ_{R3}	42
					$\delta(C_4H)$	13						$\delta(N_1C)$	26
					$\delta(C_5H)$	13	425	7	422	426	7	τ_{R2}	88
1253	34	1243	1249	30	$\nu(C_7C_8)$	10						τ_{rR}	16
					$\delta(C_4H)$	13	*g*		273	275	<1	τ_{R3}	42
					$\delta(C_2H)$	17						τ_{r2}	13
					$\delta(C_7H)$	16						$\gamma(N_1C)$	18
1204	9	1191	1197	12	$\delta(C_2H)$	33	*g*		235	236	1	$\delta(N_1C)$	56
					$\nu(N_3C_9)$	17						δ_{R3}	16
1150	7	1142	1148	4	$\delta(C_6H)$	36	*g*		224	226	1	τ_{rR}	54
					$\delta(C_7H)$	18						τ_{R2}	18
1133	1	1113	1118	<1	$\rho_1(CH_3)$	68						τ_{r1}	15
					$\rho_2(CH_3)$	23	*g*		137	138	3	$\tau(CH_3)$	57
1130	6	1116	1121	8	$\nu(C_6C_7)$	14						$\gamma(N_1C)$	19
					$\delta(C_4H)$	24	*g*		109	110	<1	$\gamma(N_1C)$	72
					$\nu(C_5H)$	18						$\tau(CH_3)$	32

[a] Experimental intensities normalized to the theoretical value for the 1534 cm^{-1} mode (140 and 86 km/mol). [b] See Table 2. [c] See Table 2. [d] See Table 2. [e] See Table 2. [f] See Table 2. [g] See Table 2.

from the diagonalization of the mass-weighted force-constant matrix were expressed in terms of the symmetry coordinates. Table 1 lists internal and symmetry coordinates for BIM and its water complexes. The potential energy distribution (PED) of the vibrational modes in terms of the internal coordinates was calculated using the standard procedure.[34] The PED matrix element, $PED_{i\rho}$, expressed in %, represents the contribution from the vibration along the ρth internal coordinate to the molecular vibration along the *i*th normal coordinate.

The H-bond interaction energy of each water complex was computed using the supermolecular approach as the difference between to total energy of the complex minus the basis-set-superposition-error-corrected (BSSE) energies of the monomers (using the so-called counterpoise method[35,36]):

$$\Delta E_{A\cdots B} = E_{A\cdots B} - E_{A(B)} - E_{B(A)} \quad (1)$$

where $E_{A\cdots B}$ is the energy of the complex, $E_{A(B)}$ is the energy

TABLE 4: (A) Ab Initio Calculated Energy Components (au), Total Energy (kJ/mol) and Dipole Moment (D) for 1:1 H-Bonded Complexes of Benzimidazole or 1-CH_3−Benzimidazole with H_2O. (B) Basis Set Superposition Error Corrected Interaction Energies (kJ/mol)[a]

		benzimidazole···H_2O			1-CH_3−benzimidazole···H_2O,
method	benzimidazole	N_1−H···OH_2	N_3···H−OH	1-CH_3−benzimidazole	N_3···H−OH
A					
MP2	−375.750 069 1	−454.995 733 8	−454.995 436 0	−417.931 191 0	−494.176 976 9
DFT	−379.893 417 0	−465.338 387 4	−456.339 118 4	−419.206 953 2	−495.653 124 3
MP+ZPE	0.114 183 2	0.137 009 8	0.137 520 2	0.140 902 8	0.164 265 7
DFT+ZPE	0.114 665 0	0.137 332 6	0.013 809 0	0.141 746 1	0.165 203 6
total MP2	−378.635 859 0	−454.858 724 0	−454.857 915 8	−417.790 288 2	−494.012 711 2
DFT	−379.778 750 0	−456.201 054 8	−456.201 093 8	−419.065 207 1	−495.487 920 7
μ(D) MP2	3.65	6.68	4.26	4.06	4.67
DFT	3.57	6.72	5.28	3.99	5.95
B					
ΔE MP2		0.00	2.12		
DFT		0.10	0.00		
MP2 (H_2O)		−76.234 389 4	−76.233 916 4		−76.234 017 4
DFT (H_2O)		−76.434 822 5	−76.434 830 4		−76.434 884 3
MP2 (base)		−378.750 713 2	−378.750 914 3		−417.932 012 1
DFT (base)		−379.893 560 3	−379.896 128 0		−419.207 146 1
interaction energy					
MP2		−29.14	−27.01		−28.05
DFT		−23.17	−23.24		−25.85
interaction energy (BSSE corrected)					
MP2		−22.59	−21.18		−22.01
DFT		−20.93	−20.87		−21.67

[a] All calculations were performed with molecular structures optimized at the MP2 or DFT 6-31++G** level.

of the monomer A obtained with the extra ghost Gaussian functions placed at the positions of the nuclei of B, and $E_{B(A)}$ is the energy of monomer B obtained with the ghost functions monomer of A.

3. Results and Discussion

3.1. Monomer Compounds in Ar. Scheme 1 illustrates the molecular structures of BIM and MBIM in their H-bonded complexes. BIM (C_s symmetry) has 39 vibrational modes: 27 A′ in-plane molecular vibrations and 12 A″ out-of-plane vibrations. In the FT−IR spectrum of monomeric BIM (see Figure 1), which is free of any water impurity or dimer absorptions, some of the absorption lines appear as doublets. Most probably matrix site effects are responsible for this phenomenon. Table 2 summarizes the experimental spectral data and the assignments made based on the calculated DFT/B3LYP frequencies and intensities. In this table and the tables which follow we only provide DFT results. Similar analysis based on the RHF calculations is available from the authors upon request.

The theoretical frequencies are scaled as described in the previous section. When a single scaling factor is used, the mean frequency deviation, $|\overline{\nu^{exp} - \nu^{theoret}}|$, is 18.7 cm^{-1} for the RHF method and 19.5 cm^{-1} for the DFT method. These values are similar to the mean deviations obtained for IM.[24] When three different scaling factors for the DFT frequencies are used (i.e., the scaling factor 0.950 for ν_{XH}, 0.980 for γ_R modes, and 0.975 for all other modes), the mean deviation decreases to 9.8 cm^{-1}. The use of different scaling factors for different types of vibrational modes has been suggested by other authors[37] and was also applied for IM.[24]

Figure 2 and Table 3 illustrate the spectral results obtained for MBIM (C_s symmetry). This molecule has 48 vibrational modes: 32 A′ in-plane vibrations and 16 A″ out-of-plane vibrations. In this case, very weak water absorptions are present in the spectrum, but they do not interfere with the assignment. The mean deviation between the experimental and theoretical frequencies in this case is 17.6 cm^{-1} for the RHF method and 19.3 cm^{-1} for the DFT method when a single scaling factor is used. Also for this compound, the mean frequency deviation decreases considerably (to 8.1 cm^{-1}) when three different scaling factors are used to scale down the DFT frequencies.

3.2. H-Bonded Complexes with H_2O. Three possible H-bonded complex structures of BIM and MBIM with water have been considered in this work: the N_1-H···OH_2 structure with BIM acting as a proton donor toward the oxygen atom of water and the two N_3···HO−H structures with BIM or MBIM acting as a proton acceptor toward one of the OH groups of water. The geometries of these complexes are shown in Scheme 1. Table 4 summarizes the results of the energy calculations for these H-bonded complexes. The calculated H-bond interaction energies for the three complexes are very similar. At the MP2//RHF level of theory, the interaction energies are −22.6, −21.2, and −22.0 kJ/mol for the BIM N_1−H···OH_2, BIM N_3···H−OH, and MBIM N_3···N−OH complexes, respectively. The DFT interaction energies are about 0.3 kJ/mol smaller for the H-bond interaction with the lone pair of the N_3 atom of BIM and MBIM and 1.7 kJ/mol smaller for the H-bond interaction at N_1−H of BIM. It can also be noted that the interaction energies for both types of complexes are very similar to those obtained for the IM water complexes.[24] These results demonstrate that both computational approaches, MP2//RHF and DFT/B3LYP, provide very similar H-bond interaction energies when the BSSE correction is accounted for. The small energy difference (only 2 kJ/mol at the MP2(BSSE)//RHF level) between the two isomeric water complexes N_1−H···OH_2 and N_3···H−OH of BIM, suggests that both complexes should be identified in the FT−IR spectra of water-doped BIM/Ar matrices.

The DFT/B3LYP calculated H-bond distances (N···O) are 2.97 and 2.90 Å for the N_1−H···OH_2 and N_3···H−OH benzimidazole water complexes, respectively. These distances are slightly shorter than those obtained at the RHF level (3.06 and 3.01 Å, respectively). The difference between the two predictions should be attributed to the correlation effects which are effectively accounted for by the DFT method.

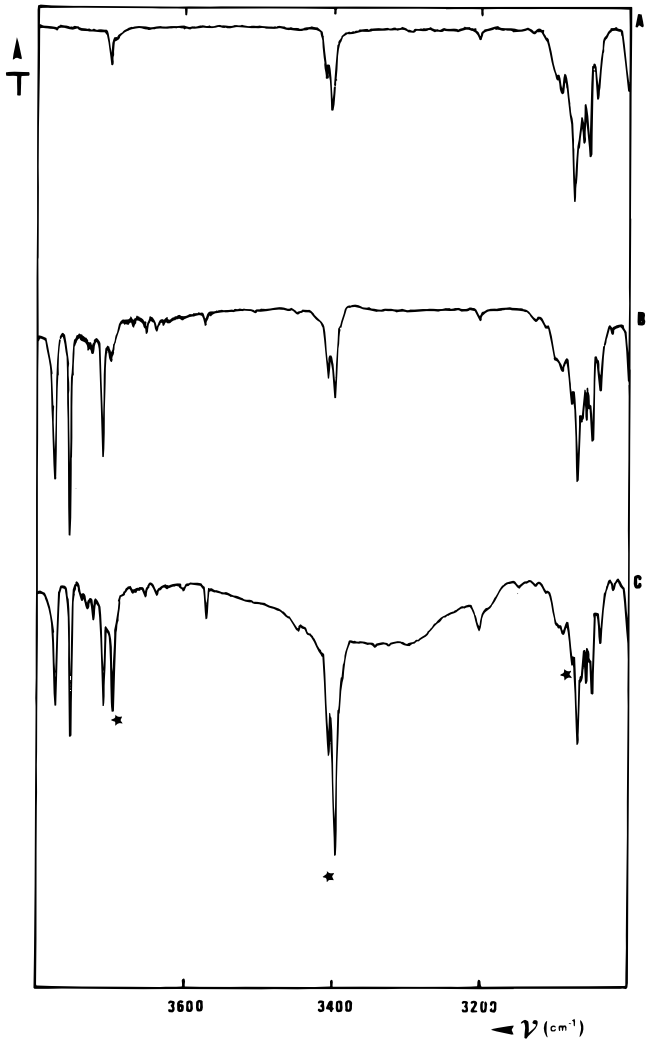

Figure 3. The $\nu_3-\nu_1$ (H_2O) region of the FT−IR spectrum of 1-CH_3−benzimidazole/H_2O/Ar (A, B, C) at 12 K (A, H_2O impurities; B, H_2O/Ar = 1/350; C, annealed spectrum of B (H_2O/Ar = 1/350); * = N···H−OH complex).

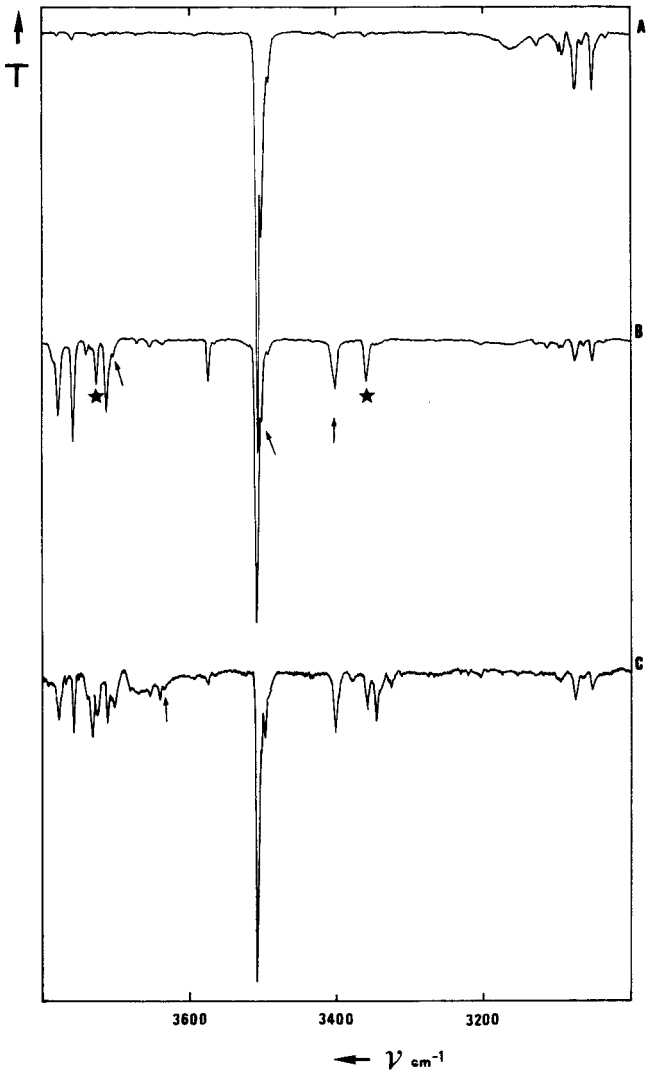

Figure 4. The $\nu_3-\nu_1$ (H_2O) and ν_{NH} region of the FT−IR spectrum of benzimidazole/Ar (A) and benzimidazole/H_2O/Ar (B,C) at 12 K (A, monomer; B, H_2O/Ar = 1/500; C, H_2O/Ar = 1/300; ↑ = N−H···OH_2 complex; * = N···HO−H complex).

The FT−IR spectra of MBIM/H_2O/Ar are shown in Figure 3. The experimental and theoretical vibrational analysis for the most perturbed (H-bond-affected) vibrational modes of the N_3···H−OH complex is summarized in Table 5. In the high-frequency region (3800−3000 cm^{-1}), a split water ν_{OH}^{b} band of the complex appears at 3409/3400 cm^{-1} when small water concentrations are used in the experiment. This mode is shifted by 238 cm^{-1} in the MBIM N_3···H−OH complex from the monomer ν_{OH}^{s} water band in Ar. When the frequency shift is approximately corrected for the difference in the vibrational coupling of the ν_3 and the ν_1 modes in free water and in H-bonded water,[38,39] the shift value becomes equal to 275 cm^{-1}. This result for the ν_{OH}^{b} mode is almost the same as the shifts observed in pyridine, 3-OH−pyridine, and IM N···H−OH H-bonded water complexes.[5−11,17,18]

Figure 4 illustrates the more complicated spectral changes in the FT−IR spectra upon complexation of BIM with water. In the $\nu_1-\nu_3$ H_2O and ν_{NH} region, one can expect two new absorptions (i.e., the absorption due to the shifted ν_{NH}... mode of the N_1−H···OH_2 complex, and the absorption due to the shifted ν_{OH}^{b}... mode of the N_3···H−OH complex. As a matter of fact, two new absorptions are observed at 3358 and 3401 cm^{-1} and these frequencies are both close to those observed for the MBIM (3400 cm^{-1}) and IM (3373 and 3394 cm^{-1}) water complexes. Similar vibrational features of water H-bonded complexes with BIM, MBIM, and IM reflect a high degree of similarity of these systems and it is consistent with the energy data discussed before.

That both the N_1−H···OH_2 and N_3···H−OH complexes are present in the Ar matrix is also manifested by the two new absorptions found in the ν_3 (H_2O) region at 3700 and 3724 cm^{-1}, though both have rather small intensities. A similar band to the former one has also been observed in the narrow spectral range of 3704−3700 cm^{-1} in FT−IR spectra of N···H−OH type water complexes of several pyridines and of IM.[5−11,24] A band similar to the latter one was found for the water complexes of 3- and 4-hydroxypyridines and IM at 3724, 3721, and 3725 cm^{-1}, respectively. In 3-hydroxypyridine, 4-hydroxypyridine, and IM water complexes the above-mentioned absorptions were attributed to the O−H···OH_2 and N−H···OH_2 H-bonded water complexes.[5−11,40,24] Although the appearance of the two pairs of bands at 3724/3700 and 3401/3358 cm^{-1} is a clear indication of the presence of the N_1−H···OH_2 and N_3···H−OH complexes, it is not obvious which of the two bands of the 3358/3401 cm^{-1} pair should be assigned to the ν_{NH}... and which to the ν_{OH}^{b} vibration, and therefore, deuteration experiments were performed to assist the assignment.

Figure 5 shows the FT−IR spectra of a matrix containing

TABLE 5: Experimental (Ar Matrix) and Calculated (DFT/6-31++G) Vibrational Data for Water and 1-CH_3−Benzimidazole in the 1:1 H-Bonded Complex N_3···HO−H**

experimental		calculated					
ν (cm^{-1})	$\Delta\nu^a$ (cm^{-1})	$\nu^{b,c}$ (cm^{-1})	$\Delta\nu^a$ (cm^{-1})	I (km/mol)	optimal scaling factor[d]	PED[e]	
water vibrations							
3699	−37	3883	−47	82	0.953	ν^f_{OH}	66
						ν^b_{OH}	34
3409/*3400*	−229/−238	3552	−241	955	0.960/0.957	ν^f_{OH}	34
						ν^b_{OH}	66
1618	+27	1644	+40	52	0.984	δ(HOH)	87
566		718		43	0.788	δ(N···HO)	72
f		374		107		δ(N···HO) oop wag[g]	83
						δ(HOH)	12
f		143		<1		ν(N−H···O)	71
f		116		116		H−O tors. about N···HO	100
f		34		1		oop butterfly	100
f		19		7		ip butterfly	100
1-CH_3−benzimidazole vibrations							
3080	+8	3153	+9	1		$\nu(C_2H)$	99
1581	+3	1580	+4	2		$\nu(C_8C_9)$	21
						$\nu(C_5C_6)$	17
						$\nu(C_4C_9)$	14
1380	+2	1354	+3	2		$\nu(C_2N_3)$	16
						$\nu(N_1C_2)$	17
1291	+3	1282	+4	33		$\nu(N_3C_9)$	30
						$\delta(C_2H)$	17
						$\delta(C_4H)$	12
						$\delta(C_5H)$	14
930?	+4	843	+5	9		$\gamma(C_2H)$	67
						$\gamma(C_7H)$	16
894	+8	879	+11	6		δ_{R1}	41
						δ_{r2}	21
						$\nu(N_3C_9)$	12
595	+7	567	+1	<1		τ_{R3}	38
						τ_{r1}	34
						τ_{R1}	38
f		105	−4	1		$\gamma(N_1C)$	54
						$\tau(CH_3)$	48

[a] Shift with respect to experimental or calculated monomer frequencies. [b] Water modes unscaled; base modes uniformly scaled. [c] Uniform scaling factor 0.97. [d] Optimal scaling factor = ν^{exp}/ν^{calc}. [e] Only contributions > 10 are listed. [f] Situated below studied region (<400 cm^{-1}). [g] oop = out-of-plane. tors. = torsional. ip = in-plane.

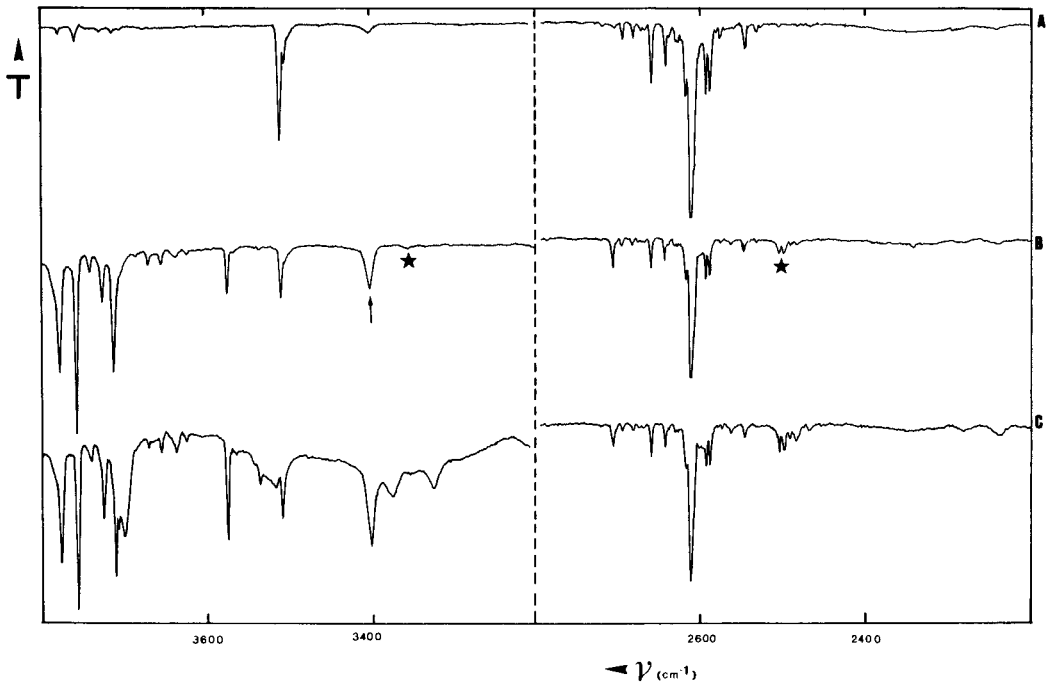

Figure 5. The $\nu_3-\nu_1$ (H_2O)/ν_{NH} (left) and ν_{ND} (right) spectral regions of the FT−IR spectrum of benzimidazole−d_1/H_2O/Ar at 12 K (A, monomer; B, H_2O/Ar = 1/350; C, annealed; ↑ = N···H−OH complex; * = N−D···OH_2 complex).

BIM-d_1 and water in the ν^b_{OH} (H_2O) and ν_{ND} regions. In the high-frequency region, the absorption at 3358 cm^{-1} almost disappeared, indicating that this absorption must originate from the ν_{N-H}... mode in the N_1−H···OH_2 complex. The absorption

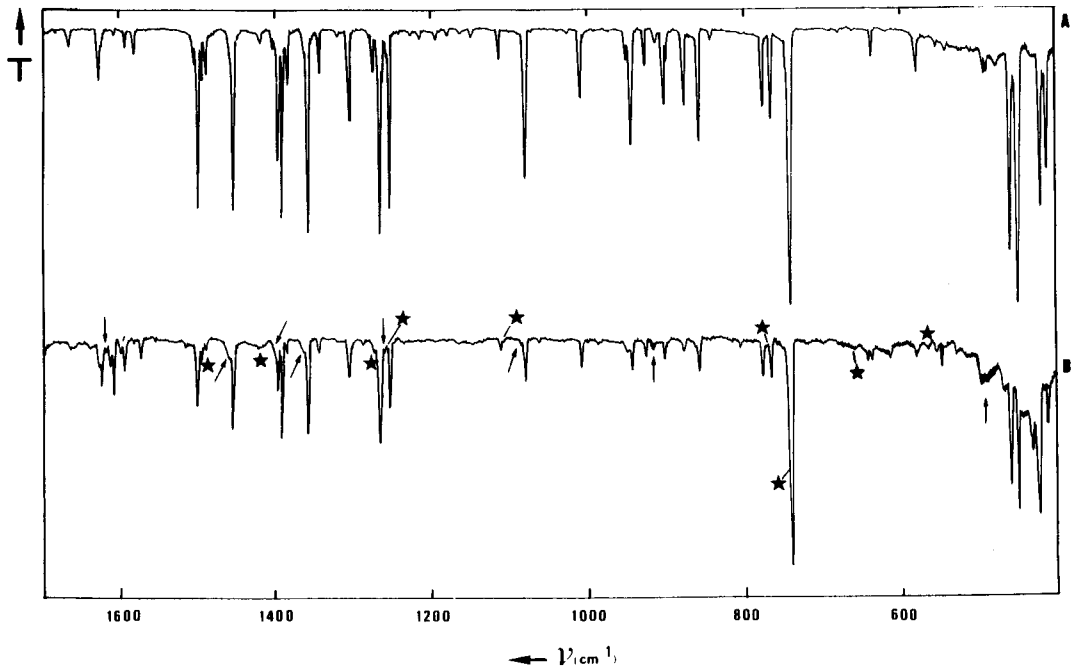

Figure 6. The effect of the H-bond complexation in the fingerprint region of the FT−IR spectrum of benzimidazole, benzimidazole/Ar (A), and benzimidazole/H_2O/Ar (B, H_2O/Ar = 1/300) at 12 K (↑ = N−H···OH_2 complex; * = N···H−OH complex).

at 3401 cm^{-1} can then be assigned to the ν_{OH}^{b} mode of the N···H−OH complex. The ν_{ND}... absorption of the deuterated-base H-bond N−D···OH_2 complex is found at 2505−2494 cm^{-1}, and the isotopic ratio, (ν_{NH}.../ν_{ND}...) of 1.34 (3358/2500), has an expected value for these rather weak complexes and is similar to the ratio found for IM.[24]

Figure 6 illustrates the perturbations of the BIM vibrational modes due to complexation with water in the fingerprint region and in the region of the water bending mode (ν_2) affected by the formation of the two H-bonded complexes. We assign the two absorptions at 1618 and 1596 cm^{-1} to the water ν_2 modes in the N_3···H−OH and N_1−H···OH_2 complexes, respectively. All the other changes in the FT−IR spectrum can be attributed to the perturbed BIM modes. The assignment of the shifted absorptions to either the N···H−OH complex or to the N−H···OH_2 complex is performed by detail comparison of the experimentally and theoretically predicted frequency shifts. Tables 6 and 7 summarize these experimental and theoretical vibrational data for the two H-bond complexes of BIM. According to the calculations, the vibrations which are sensitive to the formation of the N_1-H···OH_2 H-bond complex (i.e., the δ_{NH}... and γ_{NH}... modes) exhibit relatively large frequency shifts with respect to the monomer absorptions. In the experimental spectrum these modes are found at 1417 and 650 cm^{-1}, respectively. Large frequency shifts of these modes (25 and 201 cm^{-1}, respectively) are not predicted for the N_3···H−OH complex, and therefore, they provide an additional evidence of the coexistence of two H-bonded water complexes of BIM in the Ar matrix.

The DFT/B3LYP/6-31++G** method gives very good predictions of frequency shifts of the modes directly involved in the H-bond (e.g., the ν_{NH}... vibration of the N_1−H···OH_2 complex and the ν_{OH}^{b} vibration of the N_3···H−OH complex). The calculated values of the shifts are almost in quantitative agreement with the experimental values, and they are much better than those obtained with the RHF method. However, for the shifts of the vibrational modes involving atoms not directly participating in the H-bond interaction, the two theoretical methods give very similar qualitative predictions.

3.3. Relative Concentration of the N_1−H···OH_2 and N_3···HO-H Water Complexes of Benzimidazole. In agreement with the experimental data, the theoretically calculated relative stabilities and interaction energies for the two water complexes of BIM indicated a possible coexistence of two types of complexes in Ar matrices. The relative stability of the two complexes can be estimated from their relative concentrations in the matrix sample. With the use of the theoretically calculated intensities a and the experimental integrated intensities I of the bands at 3358 and 3401 cm^{-1}, the concentration ratio can be estimated as

$$[N_1\text{-H}\cdots OH_2]/[N_3\cdots\text{HO}-\text{H}] = (I(3358)/I(3401))(a(\nu_{OH}^{b})/a(\nu_{N_1-H\ldots}))$$

The estimated ratios calculated based on the RHF intensities and the DFT intensities of the two bands are 1.16 and 0.44, respectively. This indicates a similar abundance of the two complexes in the matrix.

3.4. Correlations between Experimental and Theoretically Predicted Parameters of N···H-OH H-Bonded Complexes. In our previous studies of H-bonded water complexes of systems modeling cytosine and isocytosine,[5−11,24] a correlation was established between the frequency shift of the ν_{OH}^{b} water mode in the N···H-OH complexes and the proton affinities (PA) of the basic N atom in the heterocyclic bases. One importance of this correlation is to estimate unknown PA values of basic N sites in polyfunctional compounds (e.g., in cytosines, adenines, or guanines). In order to use a frequency shift of the bonded-water mode ν_{OH}^{b}, in the framework of the correlation, the shift has to be corrected for the reduced vibrational coupling of the two water OH stretching modes which occurs when the complex is formed. The correction procedure was described in detail earlier.[38,39] A similar method was employed for estimating PA values from IR characteristics of H-bond complexes in inert solutions.[41]

The four-point correlation of frequency shifts and experimental PA values for IM, pyridine, pyrimidine, and 4-NH_2−

TABLE 6: Experimental (Ar Matrix) and Calculated (DFT/6-31++G) Vibrational Data for Water and Benzimidazole in the 1:1 H-Bonded Complex $N_1-H\cdots OH_2$**

experimental		calculated					
ν (cm^{-1})	$\Delta\nu^a$ (cm^{-1})	$\nu^{b,c}$ (cm^{-1})	$\Delta\nu^a$ (cm^{-1})	I (km/mol)	optimal scaling factor[d]	PED[e]	
water vibrations							
3724	−12	3929	−1	93	0.948	ν^a(HOH)	100
3632	−6	3811	−4	17	0.953	ν^a(HOH)	100
1596	+4.5	1622	+22	89	0.983	δ(HOH)	99
f		237		23		H_2O ip wag[i]	36
						τ_{rR}	23
						τ_{R3}	20
f		75		269		H_2O oop transl.	84
						H_2 oop butterfly	13
f		143		3		ν(N−H···O)	99
f		106		1		H_2O twist	96
f		46		2		H_2O ip butterfly	96
f		29		<1		H_2O oop butterfly	87
						H_2O oop transl.	13
benzimidazole vibrations							
3358	−150	3430	−132	596	0.95	$\nu(N_1H)$	99
g		3153	−2	3		$\nu(C_2H)$	99
3074	−2	3113	−3	13		$\nu(C_4H)$	67
						$\nu(C_5H)$	22
g		3105	−1	25		$\nu(C_7H)$	37
						$\nu(C_6H)$	40
						$\nu(C_4H)$	19
g		3094	−1	13		$\nu(C_5H)$	41
						$\nu(C_7H)$	44
g		3083	−3	<1		$\nu(C_6H)$	46
						$\nu(C_5H)$	33
						$\nu(C_7H)$	17
1627	0	1618	0	9		$\nu(C_7C_8)$	23
						$\nu(C_4C_5)$	13
						$\nu(N_1C_2)$	13
1579	−1	1579	−1	4		$\nu(C_8C_9)$	19
						$\nu(C_4C_9)$	17
						$\nu(C_5C_6)$	15
1494	−6	1494	−1	23		$\nu(C_2N_3)$	33
						$\delta(C_2H)$	13
						$\delta(N_1H)$	14
1491	+3	1480	0	15		$\delta(N_1H)$	14
						$\nu(C_2N_3)$	33
						$\delta(C_2H)$	15
1455	+1	1442	+3	25		$\delta(C_7H)$	20
						$\delta(C_4H)$	16
						$\nu(C_8C_9)$	14
1417	+25	1402	+18	34		$\delta(N_1H)$	34
						$\delta(C_6H)$	15
h		1352	−2	25		$\nu(C_8C_9)$	15
						$\nu(C_5C_6)$	13
g		1299	+6	14		$\delta(C_5H)$	11
						$\delta(C_2H)$	17
						$\nu(C_2N_3)$	20
						$\nu(C_3C_9)$	14
1267	+2	1254	+2	35		$\nu(N_1C_8)$	19
						$\nu(N_3C_9)$	18
						$\delta(C_4H)$	15
1258	+5	1246	+7	14		$\delta(C_7H)$	19
g		1178	+4	1		δ_{R1}	17
						$\nu(N_3C_9)$	14
						$\delta(C_2H)$	17
g		1136	−2	1		$\nu(C_5C_6)$	13
						$\delta(C_7H)$	15
						δ_{R3}	31
						$\delta(C_5H)$	20
1106	+26	1100	+33	5		$\nu(N_1C_2)$	40
						$\delta(N_1H)$	10
1007	−2	1095	−4	15		$\nu(N_1C_2)$	24
g		998	−1	8		$\nu(C_5C_6)$	47
						$\nu(C_4C_5)$	15
						$\nu(C_6C_7)$	14
g		950	−2	<1		$\gamma(C_5H)$	52
						$\gamma(C_6H)$	35
						$\gamma(C_4H)$	26

TABLE 6 (Continued)

experimental		calculated					
ν (cm^{-1})	$\Delta\nu^a$ (cm^{-1})	$\nu^{b,c}$ (cm^{-1})	$\Delta\nu^a$ (cm^{-1})	I (km/mol)	optimal scaling factor[d]	PED[e]	
947	−3	914	−1	3		$\gamma(C_4H)$	38
						$\gamma(C_7H)$	32
						$\gamma(C_6H)$	34
906	+4	918	+2	7		δ_{r1}	48
						$\nu(C_8C_9)$	21
						δ_{r2}	22
878	+1	863	+1	2		δ_{R1}	53
g		845	+6	13		$\gamma(C_2H)$	72
g		832	+5	2		$\gamma(C_7H)$	28
						$\gamma(C_4H)$	21
						$\gamma(C_5H)$	14
						$\gamma(C_2H)$	31
769	+3	742	−1	54		τ_{R1}	14
						τ_{R2}	20
						$\gamma(C_6H)$	13
g		767	+1	5		δ_{R2}	16
						$\nu(C_4C_9)$	15
						$\nu(C_7C_8)$	14
						$\nu(C_8C_9)$	17
746	+4	730	+2	119		$\gamma(C_5H)$	26
						τ_{R1}	12
						$\gamma(C_6H)$	18
650	+201	757	+332	54		$\gamma(N_1H)$	36
g		610	+1	<1		δ_{R3}	29
						δ_{R2}	31
						δ_{R1}	15
g		605	−23	19		τ_{r2}	38
						τ_{R1}	29
						$\gamma(N_1H)$	10
						τ_{r1}	29
568	−10	564	−5	5		τ_{r1}	43
						τ_{R3}	35
						τ_{R1}	29
g		535	+1	<1		δ_{R3}	71
422	+2	421	+3	9		τ_{R2}	89
412	+1	409	+4	8		δ_{R3}	53
h		261	+14	10		τ_{R3}	41
						τ_{r2}	13
						H_2O ip wag	20
h		213	−3	23		τ_{tR}	43
						τ_{R2}	14
						H_2O ip wag	35

[a] Shift with respect to experimental or calculated monomer frequencies. [b] Water modes unscaled, base modes uniformly scaled. [c] Uniform scaling factor 0.97. [d] Optimal scaling factor = ν^{ext}/ν^{calc}. [e] Only contributions > 10 are listed. [f] Situated below studied region (<400 cm^{-1}). [g] Too weak to be observed experimentally or to be assigned with confidence. [h] Overlaps with a band due to the N_3···HO−H complex. [i] ip = in-plane. oop = out-of-plane. wag = wagging. tors. = torsional. transl. = translational.

pyridine obtained following the work of Lias et al.[42] can be mathematically expressed by

$$\Delta\nu^{b}_{OH} = 1795.3 \ln(0.001263 \times PA) \qquad (2)$$

The correlation is illustrated in Figure 7. The estimation procedure for unknown PA values using experimental $\Delta\nu^{b}_{OH}$ results can be illustrated by calculation of PAs of BIM and MBIM from their respective $\Delta\nu^{b}_{OH}$ values. The PA values of 922 and 923 kJ/mol are obtained. Similarly for 3-OH−pyridine, 4-OH−pyridine, and 4-NH_2−pyrimidine, one gets 920 kJ/mol, 937 kJ/mol, and 909 kJ/mol, respectively.

Previously, we have also developed another type of correlation which can be used to estimate the ν^{b}_{OH} vibrational frequencies of water in complexes involving N···H−OH H-bonds.[5−11,17,18] The method involves calculation of so-called "optimal" scaling factors (exptl/theor) which, when multiplied by the calculated value of the frequency, produces the experimental result. The value of the factor can be correlated with the experimental or predicted parameters sensitive to the strength of the H-bond interaction. We noticed that for N(O)···HO−H H-bonded complexes the deviation of this optimal scaling factor from the commonly used value of 0.9 for RHF frequencies increases with an increasing H-bond interaction energy or an increasing $\Delta\nu^{b}_{OH}$ value (e.g., 0.872 ($(H_2O)_2$) → 0.854 (pyrimidine) → 0.847 (3-OH−pyridine) (experimental value taken from ref 33) → 0.842 (pyridine) → 0.835 (4-OH−pyridine) → 0.826 (4-NH_2−pyridine). We can now update the correlation by including the data for IM, BIM, and MBIM where the optimal scaling factors are 0.842, 0.841, and 0.843, respectively. The new updated correlation curve is shown in Figure 8. It will be used in future analysis of complicated spectra of H-bonded complexes of such polyfunctional molecules as adenine, guanine, and their analogs.

Correlation curve of the optimal scaling factor for the ν^{b}_{OH} frequency and the H-bond interaction energy yields points for IM, BIM, and MBIM N···HO−H complexes which deviate from the correlation for the pyridine type N···HO−H complexes. This deviation originates from differences in the H-bonding interactions in these two types of complexes.[18] There is another indication of these differences in the ab initio predicted structural

TABLE 7: Experimental (Ar Matrix) and Calculated (DFT/6-31++G) Vibrational Data for Water and Benzimidazole in the 1:1 H-Bonded Complex N_3···HO−H**

experimental		calculated					
ν (cm^{-1})	$\Delta\nu$[a] (cm^{-1})	ν[b,c] (cm^{-1})	$\Delta\nu$[a] (cm^{-1})	I (km/mol)	optimal scaling factor[d]	PED[e]	
water vibrations							
3700	−36	3884	−46	161	0.953	ν^{f}_{OH}	67
						ν^{b}_{OH}	33
3401	−237	3560	−232	436	0.955	ν^{f}_{OH}	33
						ν^{b}_{OH}	67
1618	+27	1640	+40	67	0.986	δ(HOH)	86
547		708		152	0.772	δ(N···HO)	79
						N···HO oop wag[i]	19
f		377		145		N···HO oop wag	73
						δ(N···HO)	13
f		146		<1		ν(N−H···O)	97
f		107		140		H−O tors. about N···HO	100
f		34		1		oop butterfly	101
f		19		12		ip butterfly	100
benzimidazole vibrations							
3498	−10	3561	−1	74	0.953	ν(N_1H)	100
3079	−14	3165	+10	2		ν(C_2H)	99
g		3118	+2	9		ν(C_4H)	62
						ν(C_5H)	26
3054	−10	3109	+3	17		ν(C_6H)	47
						ν(C_7H)	24
						ν(C_4H)	25
g		3098	+3	10		ν(C_7H)	45
						ν(C_5H)	44
g		3089	+3	<1		ν(C_6H)	43
						ν(C_5H)	25
						ν(C_7H)	29
1634	+7	1620	+2	8		ν(C_7C_8)	24
						ν(C_4C_5)	13
1581	+1	1582	+2	3		ν(C_8C_9)	20
						ν(C_4C_9)	17
						ν(C_5C_6)	15
						ν(C_6C_7)	10
		1497	+2	49		ν(C_2N_3)	54
						δ(C_2H)	20
g		1483	+3	2		δ(C_5H)	24
						ν(C_4C_5)	15
1457	+3	1442	+3	22		δ(C_7H)	22
						δ(C_4H)	19
						ν(C_8C_9)	16
1400	+8	1387	+3	37		δ(N_1H)	31
						ν(N_1C_2)	12
						δ(C_6H)	17
1360	+3	1351	+5	29		ν(C_8C_9)	15
g		1302	+1	9		δ(C_5H)	12
						ν(N_3C_9)	15
						δ(C_2H)	18
						ν(C_2N_3)	17
1262	−3	1254	+2	34		ν(N_1C_8)	16
						ν(N_3C_9)	14
						δ(C_4H)	18
1267	+14	1241	+2	15		δ(C_7H)	18
g		1171	+1	2		δ_{R1}	18
						ν(N_3C_9)	12
						δ(C_2H)	20
						ν(N_1C_8)	12
1112	−36	1140	+2	1		δ(C_6H)	29
						ν(C_5C_6)	13
						δ(C_7H)	14
						δ(C_5H)	21
g		1101	+3	2		ν(C_4C_5)	15
						δ(C_5H)	13
						δ(C_4H)	11
						δ_{R1}	14
1085	+5	1081	+14	19		ν(N_1C_2)	54
						δ(N_1H)	26
						δ(C_2H)	13
g		954	+2	<1		γ(C_5H)	53
						γ(C_6H)	38
						γ(C_4H)	28

TABLE 7: (continued)

experimental		calculated					
ν (cm^{-1})	$\Delta\nu^a$ (cm^{-1})	$\nu^{b,c}$ (cm^{-1})	$\Delta\nu^a$ (cm^{-1})	I (km/mol)	optimal scaling factor[d]	PED[e]	
g		1000	+1			$\nu(C_5C_6)$	45
		6				$\nu(C_4C_5)$	15
						$\nu(C_6C_7)$	15
h		917	+1			$\gamma(C_4H)$	39
		2				$\gamma(C_7H)$	29
						$\gamma(C_6H)$	35
916	+14	844	+5			$\gamma(C_2H)$	79
		11					
g		925	+9	3		δ_{r1}	45
						$\nu(C_8C_9)$	21
						δ_{r2}	24
h		832	+5	1		$\gamma(C_7H)$	33
						$\gamma(C_4H)$	24
						$\gamma(C_5H)$	14
						$\gamma(C_2H)$	25
g		865	+3	4		δ_{R1}	54
						$\nu(N_3C_9)$	11
h		731	+3			$\gamma(C_6H)$	17
		58				$\gamma(C_7H)$	10
						$\gamma(C_5H)$	27
						τ_{R1}	16
						$\delta(N_1H)$	14
g		768	+2			δ_{R2}	16
		8				$\nu(C_4C_9)$	15
						$\nu(C_7C_8)$	14
						$\nu(C_8C_9)$	15
h		744	+1			τ_{R1}	39
		30				τ_{r2}	29
						$\gamma(C_6H)$	15
g		628	0	5		τ_{r1}	55
						τ_{r2}	33
g		613	+4	<1		δ_{R3}	31
						δ_{R2}	28
						δ_{r1}	16
579	+1	569	0			τ_{R3}	40
						τ_{R1}	46
						τ_{r1}	20
g		535	+1			δ_{R2}	70
		<1					
493/488	+34/+39	448	+23			$\gamma(N_1H)$	97
		90					
412	−8	418	0			τ_{R2}	88
		15				τ_{rR}	14
422	+11	408	+3			δ_{R3}	49
		5					
g		248	+1			τ_{R3}	60
						τ_{r2}	17
						τ_{r1}	16
g		217	+1			τ_{tR}	69
		11				τ_{R2}	23

[a] See Table 6. [b] See Table 6. [c] See Table 6. [d] See Table 6. [e] See Table 6. [f] See Table 6. [g] See Table 6. [h] See Table 6. [i] ip = in-plane. oop = out-of-plane. wag = wagging. tors. = torsional.

parameters. The predicted distances between the hydrogen atom of water involved in the H-bond and the hydrogen atoms at carbon atoms vicinal to the H-bonded nitrogen atom in the ring are significantly smaller in the case of the complexes with the five-member-ring compounds, IM, BIM, and MBIM, than in complexes involving six-member-ring compounds (i.e., pyridines). This happens even for systems with very similar $\Delta\nu^b_{OH}$ and PA values. The difference between five- and six-member rings in H-bond interactions was further analyzed with the use of the Kitaura and Morokuma decomposition scheme in our recent work.[18]

3.5. Correlations between Experimental and Complex Parameters for X−H···OH$_2$ H-Bonded Complexes. In order for the correlation curves, such as these shown in Figures 7 and 8, to be useful in assigning the IR spectra of H-bonded polyfunctional compounds, such as the nucleic acid bases, correlations for H-bonds other than the N···HO−H or O···HO−H types should be developed. This development has started with the experimental and theoretical studies of the N$_1$−H···OH$_2$ complexes of pyrrole and[43] IM,[24] and has continued in the present work on BIM and MBIM. The results for these systems can be compared to similar results obtained for other H-bonded complexes of the X−H···OH$_2$ type, (i.e., O−H···OH$_2$ complexes such as in the water dimer, (H$_2$O)$_2$,[44] and hydroxypyridines···H$_2$O,[8] or H−NH···OH$_2$ complexes such as in aminopyri(mi)dines···H$_2$O).[7] Table 8 provides a summary of the relevant data for all the above-mentioned systems.

In Figure 9 we present the correlation curve between the experimental relative frequency shifts, $\Delta\nu_{XH\cdots}/\nu^o_{XH}$, and the ab initio calculated H-bond interaction energies. Although the number of systems of each H-bond type, (i.e., O−H···OH$_2$, N−H···OH$_2$, and H−N−H···OH$_2$) is too limited to draw

TABLE 8: Survey of Experimental and ab Initio Predicted Complex Parameters for A−H···OH_2 Complexes of Water with Different Acids

H-bonded complex	$\Delta\nu_{XH...}/\nu^{o}_{XH}$	optimal scaling for ν_{XH} and $\nu_{XH...}$ and ratio of both		MP2/BSSE+ZPE/RHF/6-31++G** H-bond energy (kJ/mol)	ref
HO−H···OH_2	0.0244	0.877/0.872	0.994	−12.17	40
3-OH−pyridine O−H···OH_2	0.0554	0.865/0.840	0.971	−23.12	7
4-OH−pyridine O−H···OH_2	0.0585	0.867/0.842	0.971	−24.74	7
pyrrole N−H···OH_2	0.0284	0.895/0.884	0.988	−18.30	this work
imidazole N−H···OH_2	0.0363	0.891/0.877	0.984	−21.72	this work
4-NH_2−pyridine H−N−H···OH_2	0.0129[a]	0.898_5[c]/0.895	0.997	−14.54	6
4-NH_2−pyrimidine H−N−H···OH_2	*b*	0.896[b,c]	−16.26	6	

[a] Shift corrected for reduced coupling in the asymmetrically bonded NH_2 group.[41] [b] In view of the large excess of the closed HN−H···OH···N species in the matrix, experimental $\nu_{XH...}$ values were only tentatively assigned for the open H−N−H···OH_2 species.[6] [c] Mean value for the modes $\nu^{a}(NH_2)$ and $\nu^{s}(NH_2)$.

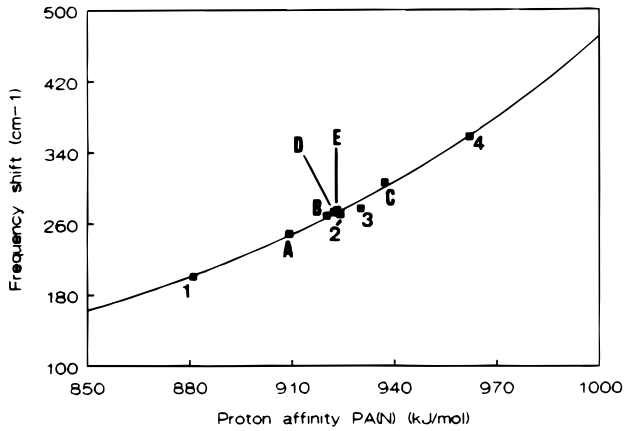

Figure 7. Correlation between the experimental water frequency shift $\Delta\nu^{b}_{OH}$ and the proton affinity of the aromatic N atom in N···HO−H complexes (1, pyrimidine; 2, pyridine; 3, imidazole; 4, 4-NH_2−pyridine; PA estimations A, 4-NH_2−pyrimidine; B, 3-OH-pyridine; C, 4-OH−pyridine; D, benzimidazole; E, 1-CH_3−benzimidazole).

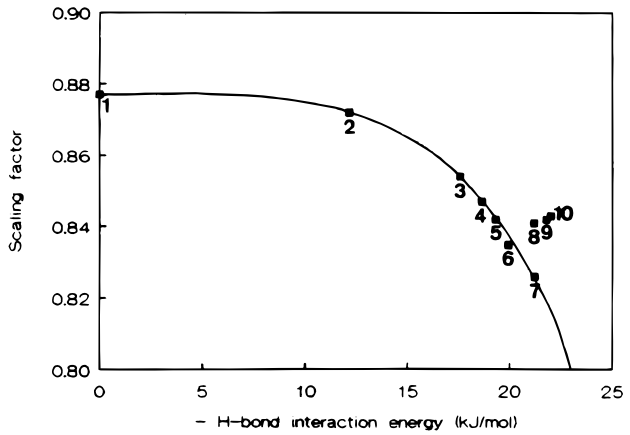

Figure 8. Correlation between the optimal scaling factor $\nu^{exp}/\nu^{theoret}$ of the water ν^{b}_{OH} mode and the predicted H-bond interaction energy for B···HO−H complexes (1, free water; 2, $(H_2O)_2$; 3, pyrimidine···H_2O; 4, 3-OH−pyridine···H_2O; 5, pyridine···H_2O; 6, 4-OH−pyridine···H_2O; 7, 4-NH_2−pyridine···H_2O; 8, benzimidazole···H_2O; 9, imidazole···H_2O; 10, 1-CH_3−benzimidazole···H_2O).

definite conclusions, it appears that each type of H-bond requires a different correlation relation. This is because the relative frequency shift at a constant interaction energy depends strongly on the type of the H-bond and decreases in the order O−H > N−H > NH_2, which follows the commonly known acidity order of these groups.[45]

We also examined the changes of the $\nu^{exp}/\nu^{theoret}$ ratio for the X−H··· mode affected by an H-bond as a function of increasing H-bond strength in a series of different X−H compounds interacting with the same proton acceptor. The

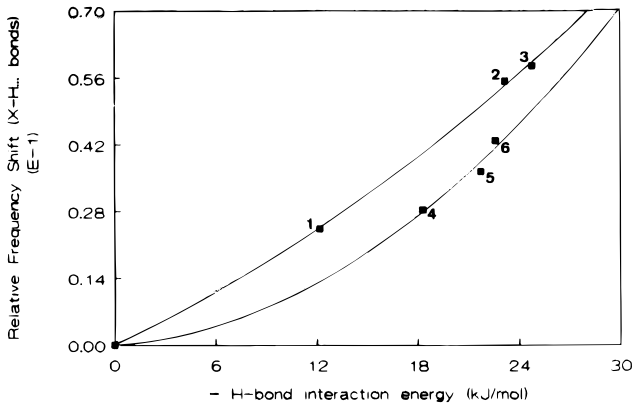

Figure 9. Correlation between the relative frequency shift $\Delta\nu_{XH...}/\nu^{o}_{XH}$ and the predicted H-bond interaction energy for X−H···OH_2 complexes (1, $(H_2O)_2$; 2, 3-OH−pyridine···OH_2; 3, 4-OH−pyridine···OH_2; 4, pyrrole···OH_2; 5, imidazole···OH_2; 6, benzimidazole···OH_2; 7, 4-NH_2−pyridine···OH_2).

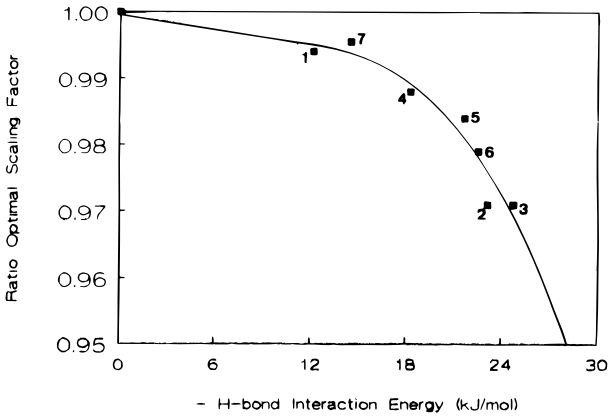

Figure 10. Correlation between the ratio of the optimal scaling factor $\nu^{exp}/\nu^{theoret}$ of the bonded and the free ν_{XH} mode and the predicted H-bond interaction energy for X−H···OH_2 complexes (numbering as in Figure 9).

difficulty with establishing a correlation in this case arises due to different degree of anharmonicity in the monomer OH, NH, and NH_2 stretching modes, leading to different $\nu^{exp}/\nu^{theoret}$ ratios already for monomeric systems with the XH modes unperturbed by H-bonding (see Table 8). This problem can be eliminated by taking as the correlated quantity not the scaling factors but the ratios of the scaling factors for the $\nu_{XH...}$ mode in the H-bonded system the scaling factors for the ν_{XH} mode of the monomer. Figure 10 demonstrates that this ratio decreases smoothly as a function of the H-bond strength, and this correlation will be more useful in future assignments of H-bonded XH stretching modes of complexes involving cytosines, adenines, and guanines.

4. Summary

In this work, the interaction between H_2O and benzimidazole and 1-CH_3−benzimidazole was investigated using FT−IR matrix-isolation spectroscopy and theoretical calculations. Benzimidazoles were selected for the study because they share the five-member-ring fragment with adenine and have no H-bonding sites in the six-member ring. This allows studies of H-bonding properties of only the five-member-ring fragment. The experiments and theoretical calculations performed in this work concern H-bonded complexes of BIM and MBIM with a single water molecule. We have investigated the vibrational and energetic parameters of these systems.

First, we performed a theoretically assisted analysis of the vibrational spectra of the monomeric BIM and MBIM in order to identify and assign the modes, which are expected to be sensitive to H-bonding interactions. In the next step these modes were used as probes for the identification of the H-bond complex type. The IR frequencies have been calculated with the RHF and DFT method.

On the basis of calculated H-bond interaction energies and on the spectral assignment for the modes sensitive to the H-bond interaction, the following three H-bond water complexes were identified: MBIM complex with H_2O at the lone pair of the N_3 atom, BIM complex with H_2O at N_1−H, and at N_3 sites. As a result of this assignment, the spectral signature of each of the three complexes was described. This information will be used in the future study of H-bonding properties of adenine.

The DFT predicted frequency shifts for the vibrational modes directly involved in the H-bond interaction are much more accurate than those obtained with the RHF method. Particularly, when three different scaling factors were applied to the DFT frequencies, a very good agreement was obtained between the experimental and theoretically predicted spectra. This agreement was instrumental in assigning the spectra. For the other vibrational modes the two theoretical methods give predictions with similar accuracy.

Finally, the experimental and theoretical data obtained in these and previous studies allowed us to derive correlations between certain experimental and calculated parameters such as frequency shifts, H-bond interaction energies, proton affinities, etc. These correlations, which can be expressed in mathematical form, will be utilized in interpretation of FT−IR spectra of matrix-isolated water complexes of adenines and adenine model molecules. For example, on the basis of the correlation curve between frequency shifts of the ν_{OH}^{b} water mode and proton affinities established for several H-bonded complexes, the proton affinities of BIM and MBIM were estimated as 922 and 923 kJ/mol, respectively.

5. Acknowlegment

The cooperation between the research groups of Leuven and Tucson was supported by the NATO International Collaborative Grant INT-9313268. G. Maes acknowledges the Flemish FWO for a permanent research fellowship, as well as the ECC for financial support (S&T cooperation with Central and Eastern European Countries research project (Grant ERB CIPA-CT93-0108)). K. Schoone acknowledges the financial support from the Flemish FWO.

References and Notes

(1) Saenger, W. *Principles of Nucleic Acid Structure*; Springer: New York, 1984.

(2) Cantor, C. R. *Biophysical Chemistry Part 1: The Conformation of Biological Macromolecules*; W. H. Freeman: San Francisco, 1980.

(3) Löwdin, P. O. *Adv. Quantum Chem.* **1965**, *2*, 213.

(4) Crick, F. H. C. *J. Mol. Biol.* **1966**, *19*, 548.

(5) Smets, J.; Adamowicz, L.; Maes, G. *J. Mol. Struct.* **1994**, *322*, 113.

(6) Destexhe, A.; Smets, J.; Adamowicz, L. Maes, G. *J. Phys. Chem.* **1994**, *98*, 1506.

(7) Smets, J.; Adamowicz, L.; Maes, G. *J. Phys. Chem.* **1995**, *99*, 6387.

(8) Buyl, F.; Smets, J.; Maes, G.; Adamowicz, L. *J. Phys. Chem.* **1995**, *99*, 14697.

(9) Smets, J. Adamowicz, L. Maes, G. *J. Phys. Chem.* **1996**, *100*, 6434.

(10) Smets, J.; Destexhe, A.; Adamowicz, L.; Maes, G. *J. Phys. Chem.* **1997**, *101*, 6583.

(11) Smets, J.; Destexhe, A.; Adamowicz, L.; Maes, G. *J. Phys. Chem.* Submitted for publication.

(12) Kwiatkowski, J. S.; Leszczynski, J. *J. Phys. Chem.* **1995**, *96*, 10094.

(13) Held, A.; Pratt, D. W. *J. Am. Chem. Soc.* **1993**, *115*, 9708.

(14) Del Bene, J. E. *J. Phys. Chem.* **1994**, *98*, 5902.

(15) Barone, V.; Adamo, C. *J. Phys. Chem.* **1995**, *99*, 15062.

(16) Sobolewski, A. L.; Domcke, W. In *The Reaction Path in Chemistry: Current Approaches and Perspectives; Ab-initio Studies of Reaction Paths in Excited-State Hydrogen-Transfer Processes*; Mezey, P. G., Ed.; Kluwer Academic Publishers: Dordrecht, 1995; pp 257−282.

(17) Maes, G. H.; Smets, J.; Adamowicz, L. In *Combined Matrix-Isolation FT−IR and Ab-initio 6-31++G** Studies on the Tautomerism and Hydrogen-Bonding Properties of Nucleic Acid Bases and Simpler Model Molecules*; Fausto, R., Ed.; NATO ASI C: *Mathematical and Physical Sciences 483*; Kluwer Academic Publishers: Dordrecht, 1996, p 147.

(18) Smets, J.; McCarthy, W.; Maes, G.; Adamowicz, L. *J. Mol. Struct. (THEOCHEM)* **1998**. Submitted for publication.

(19) Pullman, B.; Pullman, A. *Heterocycl. Chem.* **1971**, *13*, 77.

(20) Nowak, M. J.; Lapinski, L.; Kwiatkowski, J. S.; Leszczynski, J. *Spectrochim. Acta A* **1991**, *47*, 87. Nowak, M. J.; Lapinski, L.; Kwiatkowski, J. S.; Leszczynski, J. *J. Am. Chem. Soc.* **1998**. Submitted for publication.

(21) Nowak, M. J.; Rostkowska, H.; Lapinski, L.; Kwiatkowski, J. S.; Leszczynski, J. *J. Phys. Chem.* **1994**, *98*, 2813.

(22) Houben, L. Ph.D. thesis, University of Leuven, 1998. In preparation.

(23) Ramaekers, R.; M.S. Thesis, University of Leuven, 1996.

(24) Van Bael, M. K.; Schoone, K.; Houben, L.; Smets, J.; McCarthy, W.; Adamowicz, L.; Nowak, M. J.; Maes G. *J. Phys. Chem.* **1997**, *101*, 2397.

(25) Mohan, S.; Sundaragan, J.; Mink, J. *Thermochim. Acta A*, **1991**, *47*, 1111.

(26) Suwaiyan, A.; Zwarich, R.; Baig, N. *J. Raman Spectrosc.* **1990**, *21*, 243.

(27) Maes, G. *Bull. Soc. Chim. Belg.* **1981**, *90*, 1093.

(28) Graindourze, M.; Smets, J.; Zeegers-Huyskens, Th.; Maes, G. *J. Mol. Struct.* **1990**, *222*, 345.

(29) Schoone, K. M.S. Thesis, University of Leuven, 1995.

(30) Chalasinski, G.; Szczesniak, M. *Chem. Rev.* **1994**, *94*, 1723.

(31) Becke, A. D. *J. Chem. Phys.* **1993**, *98*, 5648.

(32) Parr, R. G.; Yang, W. *Density-Functional Theory of Atoms and Molecules*; Oxford University Press: New York, 1989.

(33) Frisch, C. P M. J.; Trucks, G. W.; Head-Gordon, M.; Gill, P. M. W.; Wong, W. M.; Foresman, J. B.; Johnson, B. G.; Schlegel, H. B.; Robb, M. A.; Replogie, E. S.; Gomperts, R.; Andres, J. L.; Raghavachari, K.; Binkley, J. S.; Gonzales, C.; Martin, R. L.; Fox, D. J.; Defrees, D. J.; Baker, J.; Stewart, J. J. P.; Pople, J. A. GAUSSIAN 92; Gaussian, Inc.: Pittsburgh, PA, 1992. Frisch, C. P M. J.; Trucks, G. W.; Schlegel, H. B.; Gill, P. M. W.; Johnson, B. G.; Robb, M. A.; Cheeseman, J. R.; Keith, T.; Petersson, G. A.; Montgomery, J. A.; Raghavachari, K.; Al-Laham, M. A.; Zakrzewski, V. G.; Ortiz, J. V.; Foresman, J. B.; Peng, C. Y.; Ayala, P. Y.; Chen, W.; Wong, M. W.; Andres, J. L.; Replogle, E. S.; Gomperts, R.; Martin, R. L.; Fox, D. J.; Binkley, J. S.; Defrees, D. J.; Baker, J.; Stewart, J. P.; Head-Gordon, M.; Gonzales, C.; Pople, J. A. GAUSSIAN 94, Revision B.3; Gaussian, Inc.: Pittsburgh, PA, 1995.

(34) Califano, S. *Vibrational States*; Wiley: New York, 1976.

(35) Boys, S. F.; Benardi, F. *Mol. Phys.* **1970**, *19*, 553.

(36) Van Duijneveldt, F. B.; van Duijneveldt-van de Rijdt, J. G. C. M.; van Leuthe, J. H. *Chem. Rev.* **1994**, *94*, 1873.

(37) Rauhut, G.; Pulay, P. *J. Phys. Chem.* **1995**, *99*, 309.

(38) Schiöberg, D.; Luck, W. A. P. *J. Chem. Soc., Faraday Trans.* **1979**, *1*, 762.

(39) Maes, G.; Smets, J. *J. Mol. Struct.* **1992**, *270*, 141.

(40) Person, W. B.; Del Bene, J. E.; Sajda, W.; Szczepaniak, K.; Szczesniak, M. *J. Phys. Chem.* **1991**, *95*, 2770.

(41) Goethals, M.; Platteborze, K.; Zeegers-Huyskens, Th., *Spectrochim. Acta* **1992**, *48A*, 671.

(42) Lias, S. G.; Liebman, J. F.; Levin, R. D. *J. Phys. Chem. Ref. Data* **1984**, *13*, 695.

(43) Van Bael, M. K. M.S. Thesis, University of Leuven, 1994.

(44) Engdahl, A.; Nelander B. *J. Mol. Struct.* **1989**, *193*, 101.

(45) Perrin, D. D. *Dissociation Constants of Organic Bases in Aqueous Solution*; Butterworths: London, 1965.